

# Doping of a One-Dimensional Mott Insulator: Photoemission and Optical Studies of $\text{Sr}_2\text{CuO}_{3+\delta}$

T. Valla,\* T. E. Kidd, P. D. Johnson, K. W. Kim,<sup>†</sup> C. C. Homes, and G. D. Gu  
*Department of Physics, Brookhaven National Laboratory, Upton, NY, 11973-5000*

(Dated: March 22, 2022)

The spectral properties of a one-dimensional (1D) single-chain Mott insulator  $\text{Sr}_2\text{CuO}_3$  have been studied in angle-resolved photoemission and optical spectroscopy, at half filling and with small concentrations of extra charge doped into the chains via high oxygen pressure growth. The single-particle gap is reduced with oxygen doping, but the metallic state is not reached. The bandwidth of the charge-transfer band increases with doping, while the state becomes narrower, allowing unambiguous observation of separated spinon and holon branches in the doped system. The optical gap is not changed upon doping, indicating that a shift of chemical potential rather than decrease of correlation gap is responsible for the apparent reduction of the photoemission gap.

PACS numbers: 71.27.+a, 78.20.Bh, 79.60.Bm

1D Mott insulators have been intensively studied both theoretically and experimentally because of the fundamentally different physics expected in 1D [1]. Systems with nearly non-interacting Cu-O chains, for example, represent an ideal realization of a Heisenberg spin 1/2 chain [2]. Early on, it was realized that in 1D systems the elementary electronic excitations are not quasiparticles (QP) as in 3D systems, but collective excitations carrying either spin but no charge ("spinons") or the charge of an electron but no spin ("holon") [3]. If created in such a system, a physical electron (or hole) decays into a pair of independent excitations. A photoemission spectrum that measures the spectral function of a physical hole is therefore a broad multi-particle continuum of spinons and holons. Similarly, in inelastic neutron scattering (INS) that measures the spin-spin correlation function, a two-spinon continuum is expected instead of well-defined magnons. The boundaries of the continuum, representing events where one particle is left at rest, may still be well pronounced and it should be possible to trace the spinon and holon branches in photoemission, and lower and upper boundaries in INS [4, 5]. While the boundaries of the continuum have been identified in neutron scattering [6, 7], the spinon and holon branches have not been resolved as clearly in photoemission [8]. Theoretical studies suggest that the direct observation of spinon-holon branches is more likely in insulating 1D materials [9]. These systems, with partially filled valence bands, are insulators due to the strong electronic correlations that forbid double occupancy of sites. In the "spin-charge separated" picture, charge excitations (holons) are gapped, while the spinons may be gapless and form a "Fermi surface". Gapping of the charge excitations partially suppresses blurring of the branches, raising the chances for their direct observation.

In this letter, we show that the material with a single chain per unit cell,  $\text{Sr}_2\text{CuO}_3$ , may be doped with holes when grown in a high oxygen pressure. The single particle gap is significantly reduced with doping, while the op-

tical gap remains nearly constant, the system remaining in an insulating state. Sharpening of the charge transfer state and its increased dispersion in doped samples enables unambiguous detection of the spinon and holon branches in the raw data for the first time.

The photoemission experiments were carried out on a high-resolution photoemission facility based on undulator beam-line U13UB at the National Synchrotron Light Source with a Scienta SES-200 electron spectrometer. The combined instrumental energy resolution was set to  $\sim 25$  meV. The angular resolution was better than  $\pm 0.1^\circ$  translating into a momentum resolution of  $\pm 0.0025 \text{ \AA}^{-1}$  at the 15.2 eV photon energy used in the study. The large single crystals were grown by traveling solvent-floating zone method under different oxygen pressure. For photoemission studies, samples were mounted on a liquid He cryostat and cleaved *in-situ* in the UHV chamber with base pressure  $3 \times 10^{-9}$  Pa. The polarized reflectance of freshly-cleaved crystals of  $\text{Sr}_2\text{CuO}_{3+\delta}$  were measured over a wide frequency range ( $\sim 30$  to over  $23,000 \text{ cm}^{-1}$ , or 3 meV to  $\sim 3$  eV) on a Bruker IFS 66v/S Fourier transform spectrometer using an overfilling technique [10]. The principal optical axes were determined from the anisotropic behavior of the phonons; a prominent copper-oxygen stretching mode at  $\sim 540 \text{ cm}^{-1}$  is observed only along the chain direction ( $b$  axis). The optical properties were then calculated from a Kramers-Kronig analysis of the reflectance.

Fig. 1a) shows the photoemission intensity for  $\text{Sr}_2\text{CuO}_{3+\delta}$  grown under 5.5 bar of  $\text{O}_2$ , measured along the chain direction,  $k_b$ , with the in-plane momentum perpendicular to the chains set to  $k_a = 0$ . The dispersion of the lower Hubbard band (or more correctly - the charge transfer band) gapped by a large correlation gap is clearly visible. The state disperses upwards for  $k < k_F$ , achieves a maximum at  $k = k_F$  and then turns down for  $k > k_F$ . In Fig. 1b), the intensity at fixed  $k = k_F \approx \pi/(2b)$  (the so called energy distribution curve (EDC)) is plotted for three different growth conditions. It is obvious

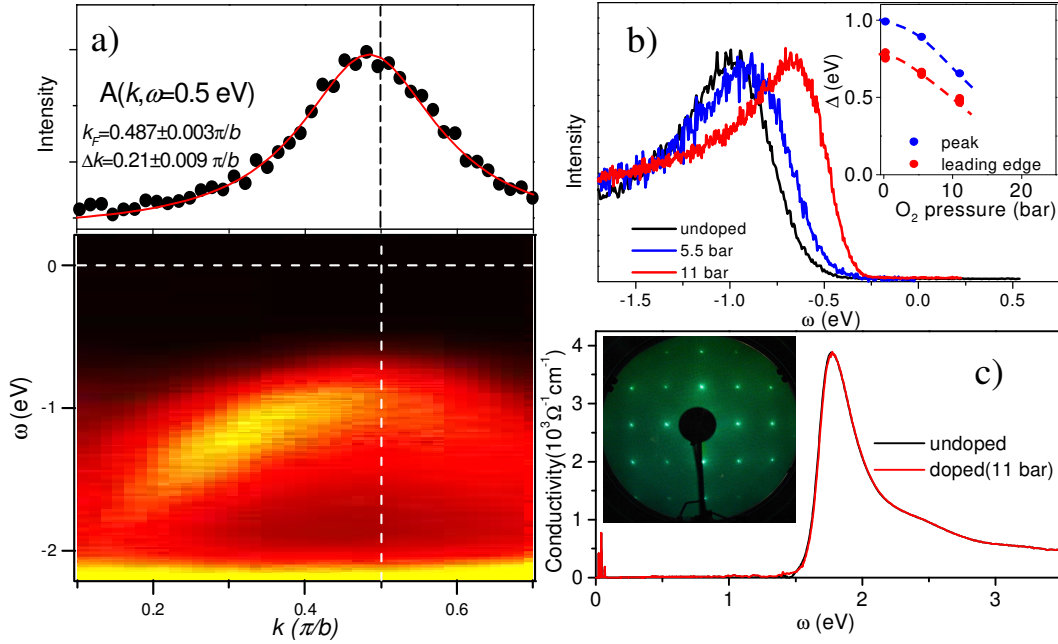


FIG. 1: a) Photoemission intensity of 5.5 bar sample in the chain direction. Lower panel shows false color contour map with highest intensity in yellow. The dashed lines represent  $\omega = 0$  and  $k = \pi/(2b)$ . Upper panel represents the cross-section of the same spectrum (MDC) at  $\omega = 0.5$  eV. The red line is Lorentzian fit to the data. b) Photoemission spectra at  $k_F$  for three different growth conditions of  $\text{Sr}_2\text{CuO}_{3+\delta}$ . Spectra were recorded at 200K (doped) and 300 K (undoped) samples. Inset: the single-particle gap dependence on  $\text{O}_2$  growth pressure. c) Optical conductivity at room temperature for light polarized along the  $b$  axis (chain direction) for the undoped and 11 bar  $\text{O}_2$  grown samples. Inset: LEED pattern for 11 bar sample at 164 eV electron energy.

that the gap magnitude decreases with the increasing  $\text{O}_2$  growth pressure, from  $\approx 0.75$  eV for the undoped material to  $\approx 0.5$  eV for the highest growth pressure, measured as the position of the "leading edge". In the inset, we show the growth pressure dependence of the single-particle gap, which suggests that the metallic state might be reached for the  $\text{O}_2$  pressure of 20-30 bar. The obvious reduction of the photoemission single-particle gap with increasing oxygen content is in sharp contrast with the behavior observed in optical measurements.

The optical conductivity (or current-current correlation function) [11] represents an integral throughout the Brillouin zone of all the  $q = 0$  transitions. As can be seen in Fig. 1c), the optical gap remains constant upon doping. Moreover, the real part of the optical conductivity  $\sigma_1(\omega)$  does not show any significant difference for samples grown under different conditions. The photoemission gap is approximately 1/2 of the optical gap for the undoped sample but not for the 11 bar grown sample. This would suggest that the correlation gap has not changed, but rather, the chemical potential has been shifted closer to the lower Hubbard band. However, the shift is pronounced only for the highest occupied state and only near  $k_F$ . At the zone center the state does not shift with doping. Also, the deeper states shift only by a fraction of the gap reduction. The fact that the insulating character of a 1D Mott insulator is preserved

upon doping is fundamentally new and in contrast with 2D cuprates where a small concentration (1-2%) of doped carriers induces states at the Fermi level and the development of metallic in-plane transport [12].

Although the exact oxygen content is not known for our samples, we anticipate that the doping level is very low. As the structure of the cleaved surfaces, determined by LEED (Fig. 1c), inset), is the same for all the samples, the system retains its orthorhombic structure for the range of growth conditions applied here. This is consistent with the previous study on lightly-doped polycrystalline samples [13] where the insulating phase and the structure was preserved for  $\delta < 0.03$  to 0.1. That study also suggested that the extra oxygen went into the same interstitial sites in the rocksalt  $\text{Sr}(\text{La})\text{O}$  structure as in oxygen-doped  $\text{La}_2\text{CuO}_{4+\delta}$ . Such interstitial oxygen can oxidize the Cu-O chains in the same manner as it oxidizes the planes in  $\text{La}_2\text{CuO}_{4+\delta}$ . The effective doping level of Cu-O chains should then be directly measurable in photoemission, by measuring  $k_F$ . For the undoped material, the chains are half-filled, and  $k_F$  is exactly  $0.5\pi/b$ . If the chains were doped with holes, the  $k_F$  should be somewhat smaller. The upper panel in Fig. 1a) represents the momentum distribution curve (MDC) at energy  $\omega$  set inside the gap where only the "tail" of the lower Hubbard band extends. The MDC is peaked very close to  $0.5\pi/b$  for all our samples, indicating that the departure from

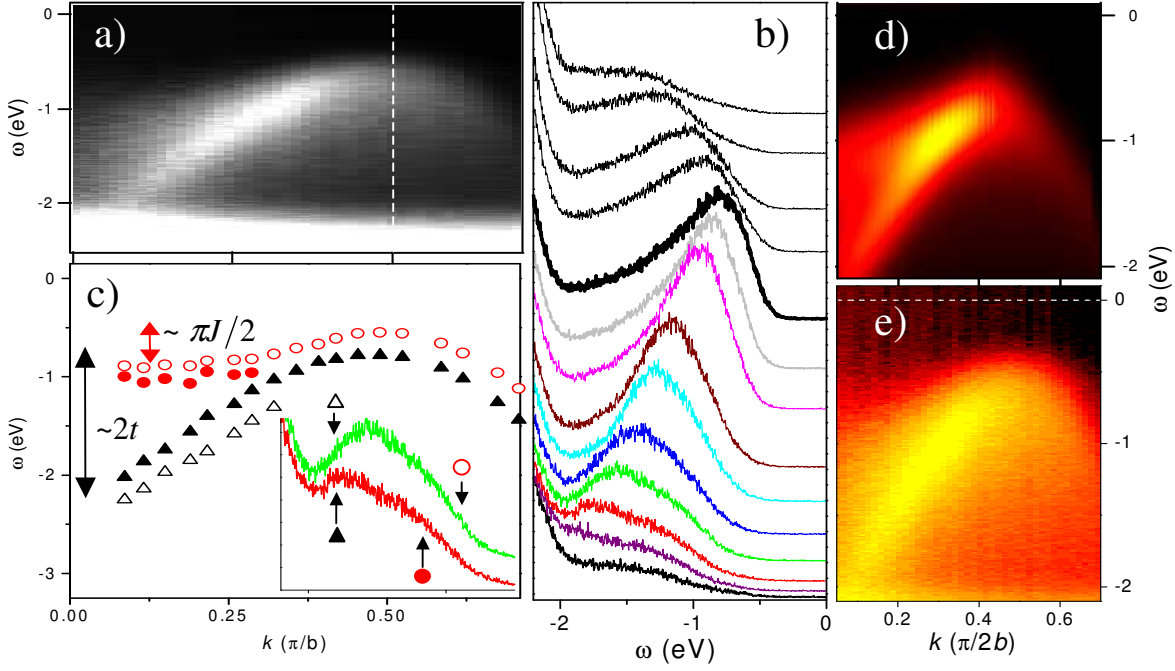


FIG. 2: a) Contour plot of photoemission intensity recorded at 180 K from a freshly cleaved 11 bar grown sample in the chain direction. The dashed line represents  $k = \pi/(2b)$ . b) A set of corresponding EDCs for several momenta, increasing from bottom to the top. The thick spectrum corresponds to  $k_F$ . c) Dispersion of characteristic features in the spectra from panel (b). Solid (empty) circles represent "full" ("middle") step on the upper (spinon) edge, while triangles represent corresponding features on the lower (holon) edge, as indicated in the inset for re-plotted 3<sup>rd</sup> and 4<sup>th</sup> EDC from the bottom in panel (b). d) The spectral function simulated as explained in the text [5]. e) The same spectrum as in a), but with intensity on a log-scale, emphasizing the spinon branch.

half-filling is smaller than or equal to the experimental uncertainty of 2-3% [14].

Another intriguing feature is an apparent sharpening of the charge transfer state with doping (see Fig. 1b)). If the additional oxygen were to introduce disorder into the Cu-O chains, the effect would be opposite. It is more probable that the charge induced from the interstitial sites helps in screening the photohole created in the photoemission process. Irrespective of the origin, the observed sharpening is found to be essential for detection of spin-charge separation in the high-pressure grown samples as discussed below.

We note that the extra oxygen tends to leave the surface area probed in photoemission relatively quickly after cleaving, shifting the probed layer closer to the undoped case. After a day in ultra-high vacuum, the spectra of an 11 bar grown sample look identical to the freshly cleaved 5.5 bar grown sample. If re-cleaved, the 11 bar characteristics are recovered reproducibly, meaning that only the surface region was affected. The loss of oxygen and its resulting inhomogeneous concentration might be a dominant factor that limits the total photoemission width of the measured states. Although the width and the gap increase in time, it is not clear what the contribution to the initial width was. However, the spectra of the high pressure grown samples were sharp enough to observe the

spin-charge separation directly in the raw data. Fig. 2a) shows the photoemission intensity in the in-chain direction from an 11 bar sample at  $T = 180$  K, within 15 minutes after cleaving. In the raw data contour plot, there is already a hint of two separated branches in the dispersion of the highest occupied state for  $k < k_F$ . In panel b), the same spectrum is shown as a set of EDCs for several different momenta. Although the dispersion may seem symmetric relative to  $k_F$ , there is a significant difference in the lineshape between the  $k < k_F$  and  $k > k_F$  regions. For  $k < \pi/(3b)$ , the spectral intensity has a complex shape in that it seems to be limited between two dispersing step-like features: a rapidly dispersing lower edge and a slowly dispersing upper edge. As these edges merge, forming a wedge-like structure, only a single-peak can be identified near  $k_F$ . A single-peak structure remains above  $k_F$ . This is exactly what is expected if spin-charge separation takes place. The rapidly dispersing lower edge represents the holon branch while the upper edge represents the spinon branch. In the cases where these two edges are well separated, one can identify the "mid-point" and the "full-step" energies for each edge, as shown in the inset of Fig. 2c), and plot them vs. corresponding momenta. In cases where only a single peak is present, we plot the peak position and the upper (leading) edge position. The results are shown in panel

c). If we identify the lower edge as the holon and the upper edge as the spinon branch, we get approximately 1.64 eV and 0.4 eV for the total holon and spinon bandwidth, respectively. In the  $t - J$  model, this corresponds to  $t = 0.82$  eV and  $J = 0.26$  eV, somewhat larger than previous estimates for an undoped system [2, 7, 15]. As noted earlier, the dominant change induced by the increasing oxygen content is the gap reduction. At the same time, the bottom of the holon branch (at  $k = 0$ ) remains nearly at the same energy ( $\sim 2.5$  eV). That means that the holon bandwidth increases with doping. By using the gap dependence on pressure, we obtain  $t \sim 0.66$  eV and 0.72 eV for the undoped and 5.5 bar grown material, respectively. We were able to resolve the spinon branch in the 5.5 bar sample, but not in the undoped system. Compared to the 11 bar sample,  $J$  is slightly reduced, but within the error of approximately  $\pm 0.05$  eV.

To the best of our knowledge, our photoemission spectra from high oxygen pressure grown  $\text{Sr}_2\text{CuO}_{3+\delta}$  provide the best direct evidence for spin-charge separation so far. The continuum of excitations, with well-resolved spinon and holon branches, have been identified from the raw data without resorting to the technique of second derivatives [16, 17]. Spurious states, dispersing in the wrong direction near the zone center and the zone boundary from ref. [16], have not been detected. To better illustrate the agreement with the theoretical models for 1D Mott insulators, we have simulated the spectral function in Fig. 2(d), by using eq. (23) from ref. [5] with  $v_c = 6v_s$  and convoluted it with an 0.4 eV gaussian. Even though the agreement is remarkable, there are still some discrepancies between our data and the theoretical models. For example, the observed asymmetry in intensity between the holon and spinon branches cannot be explained in a simple 1-band Hubbard model. Theories going beyond 1-band model seem to be able to account for an apparent weakening of the spinon branch [18]. To emphasize the lower intensity spinon component, we have replotted the experimental spectrum with a log-scale for intensity in panel (e). An additional problem is the anomalously large broadening and the "leakage" into the gap that is clearly visible in the photoemission data (Fig. 1). As spinons are gapless, the "Fermi surface" that they form will be smeared out at finite temperature. However, as recent finite temperature calculations have shown, this will affect the holon branch much more strongly, while the spinon edge will remain relatively sharp [9]. Our photoemission and optical spectra show virtually no temperature dependence, with the "leakage" still present at low temperatures.

In conclusion, we have succeeded in doping the single chain Mott insulator  $\text{Sr}_2\text{CuO}_3$  with holes via high-pressure oxygen growth. Upon doping, the single particle gap decreases while the optical gap remains constant. The  $k_F$  remains close to  $\pi/(2b)$ , indicating a very low

doping level. In doped samples, the separated spinon and holon branches have been detected. From the measured dispersions, we have deduced the set of  $t - J$  parameters that agree well with some earlier estimates [7, 15] and seem to increase with doping.

The authors would like to acknowledge useful discussions with Alexei Tsvetlik, Igor Zaliznyak, Young-June Kim and especially with Fabian Essler, who guided us through the 1D physics. The work was supported by the Department of Energy under contract number DE-AC02-98CH10886.

---

\* Electronic address: valla@bnl.gov

† Permanent address: School of Physics and Research Center for Oxide electronics, Seoul National University, Seoul 151-747, Korea

- [1] S. Maekawa and T. Tohyama, Rep. Prog. Phys. **64**, 383 (2001) and references therein.
- [2] A. Keren *et al*, Phys. Rev. B **48**, 12926 (1993); T. Ami *et al*, Phys. Rev. B **51**, 5994 (1995); N. Motoyama, H. Eisaki, and S. Uchida, Phys. Rev. Lett. **76**, 3212 (1996); K. M. Kojima *et al*, Phys. Rev. Lett. **78**, 1787 (1997).
- [3] V. J Emery, A. Luther and I Peschel, Phys Rev. B **13**, 1272 (1976); E. H. Lieb and F. Y. Wu, Phys. Rev. Lett. **20**, 1445 (1968).
- [4] A. Parola and S. Sorella, Phys. Rev. B **45**, 13156 (1992); Phys. Rev. B **57**, 6444 (1998).
- [5] F. H. L. Essler and A. M. Tsvetlik, Phys. Rev. B **65**, 115117 (2002).
- [6] D. A. Tennant, T. G. Perring, R. A. Cowley, and S. E. Nagler Phys. Rev. Lett. **70**, 4003 (1993); M. Arai *et al*, Phys. Rev. Lett. **77**, 3649 (1996).
- [7] I. A. Zaliznyak *et al*, cond-mat/0312724;
- [8] C. Kim *et al*, Phys. Rev. Lett. **77**, 4054 (1996); Phys. Rev. B **56**, 15589 (1997).
- [9] F. H. L. Essler and A. M. Tsvetlik, Phys. Rev. Lett. **90**, 126401 (2003).
- [10] C. C. Homes, M. Reedyk, D. A. Crandles, and T. Timusk, Appl. Opt. **32**, 2972 (1993).
- [11] R. Kubo, J. Phys. Soc. Japan **12**, 570 (1957); D. A. Greenwood, Proc. Phys. Soc. (London) **A71**, 585 (1958).
- [12] S. Komiya, Y. Ando, X. F. Sun, and A. N. Lavrov, Phys. Rev. B **65**, 214535 (2002); S. Uchida *et al*, Phys. Rev. B **43**, 7942 (1991); M. Dumm *et al*, unpublished; T. Yoshida *et al*, cond-mat/0206469 (2002).
- [13] W. B. Archibald, J. -S. Zhou, and J. B. Goodenough, Phys. Rev. B **52**, 16101 (1995).
- [14] Although the angular resolution allows much higher precision, the uncertainty in the work function and/or in the absolute angle may produce a 2-3% uncertainty in  $k_F$ .
- [15] H. Suzuura *et al*, Phys. Rev. Lett. **76**, 2579 (1996); R. Neudert *et al*, Phys. Rev. Lett. **81**, 657 (1998).
- [16] H. Fujisawa *et al*, Phys. Rev. B **59**, 7358 (1999).
- [17] T. Mizokawa *et al*, Phys. Rev. Lett. **85**, 4779 (2000).
- [18] K. Penc and W. Stephan, Phys. Rev. B **62** 12707 (2000).